EEET ECOLOGICAL ENGINEERING & ENVIRONMENTAL TECHNOLOGY

Ecological Engineering & Environmental Technology, 2026, 27(9), 149–162
https://doi.org/10.12912/27197050/226003
ISSN 2719–7050, License CC-BY 4.0

Received: 2026.06.26
Accepted: 2026.07.31
Published: 2026.08.15

Iron accumulation in paddy soils and rice grains exposed to acid mine drainage and its association with rice quality in Kolaka Regency, Southeast Sulawesi, Indonesia

Ansyar Tambara[1], Fahruddin Fahruddin[2*], Baharuddin Patandjengi[3]

[1] Study Program of Agricultural Sciences, Graduate School of Hasanuddin University, Jl. Perintis Kemerdekaan Km. 10, Makassar, Indonesia
[2] Department of Biology, Faculty of Mathematics and Natural Science, Hasanuddin University, Jl. Perintis Kemerdekaan Km. 10, Makassar, Indonesia
[3] Department of Pest and Plant Diseases, Faculty of Agriculture, Hasanuddin University, Jl. Perintis Kemerdekaan Km. 10, Makassar, Indonesia
* Corresponding author's e-mail: fahruddin_science@unhas.ac.id

ABSTRACT

Nickel mining activities in Kolaka Regency, Southeast Sulawesi, Indonesia, have generated acid mine drainage (AMD) that contaminates adjacent agricultural land, including the paddy fields of Pesouha Village, Pomalaa Sub-district. This study investigated the accumulation of iron (Fe) in paddy soils and rice grains across an AMD contamination gradient and evaluated its implications for rice plant growth and grain quality. Sampling was conducted at four stations positioned at increasing distances from an AMD-affected irrigation channel: station 1 (200 m), station 2 (500 m), station 3 (2 km), and station 4 as an uncontaminated control (4 km), with three independent replicate plots established per station for both soil and rice grain analyses. Fe concentrations in soil and rice grain were quantified by atomic absorption spectrophotometry, and grain quality was evaluated visually following the Indonesian National Standard (SNI 6128:2020). Soil Fe concentrations were 3.10, 2.92, 2.17, and 1.19 mg/kg at stations 1 through 4, respectively, all exceeding the permissible threshold of 0.5 mg/kg set by SNI and WHO guidelines. Grain Fe content followed a different pattern, with the highest concentration recorded at station 1 (156 mg/kg), followed by the control station 4 (115 mg/kg), station 2 (66.67 mg/kg), and station 3 (50.13 mg/kg); all values substantially exceeded the WHO/FAO safe limit of 5–10 mg/kg for food commodities. Rice plants at contaminated stations exhibited iron toxicity symptoms, including leaf chlorosis, stunted growth, impaired root development, and reduced panicle formation, whereas the control station supported the healthiest plant growth and the highest grain quality score. Pearson correlation analysis indicated a moderate positive relationship between grain Fe content and grain quality score ($r = 0.55$), although this correlation was not statistically significant ($p > 0.05$), likely reflecting the limited number of stations ($n = 4$). The observed relationships should be regarded as preliminary and require validation using a larger number of independent sampling sites. These findings illustrate the dual role of Fe as both an essential nutrient and a potential contaminant, and underscore the urgent need for continuous monitoring and management of irrigation water quality in agricultural areas adjacent to nickel mining operations.

Keywords: acid mine drainage, iron accumulation, rice quality, contaminated paddy fields, Fe toxicity.

INTRODUCTION

Nickel mining in Indonesia has expanded substantially over recent decades, particularly in Kolaka Regency, located in Southeast Sulawesi Province one of the country's most productive nickel-producing regions. The rapid advancement of the mining industry in this area poses significant risks to surrounding agricultural lands, threatening environmental quality and ultimately compromising the yield and quality of rice production (Fahruddin et al., 2021; Tambara et al., 2025a).

One of the most conspicuous environmental consequences of mining operations is the formation of acid mine drainage (AMD), which occurs when sulfide-bearing minerals, such as pyrite (FeS_2), are exposed to oxygen and water during mining activities. These oxidative reactions generate sulfuric acid and release substantial quantities of dissolved metals and sulfate ions (SO_4^{2-}) into the AMD effluent (Jiao et al., 2023; Fahruddin et al., 2024). The resultant acidic conditions promote the mobilization of heavy metals from mine rock into adjacent water bodies.

When AMD-laden irrigation water enters paddy fields, it introduces heavy metals that disrupt the agricultural ecosystem. Specifically, AMD acidifies paddy soils, elevates the concentrations of available sulfur and extractable heavy metals particularly Fe to critical levels, while simultaneously reducing the availability of phosphorus, potassium, and zinc (Titania et al., 2026). These conditions directly diminish land productivity and threaten the sustainability of rice cultivation.

Iron (Fe) is the primary heavy metal of concern in the context of paddy soil contamination by AMD. Under flooded, anaerobic, and low-pH soil conditions, ferric iron (Fe^{3+}) is reduced to the more soluble ferrous form (Fe^{2+}). Excess ferrous ions are subsequently absorbed by roots and transported via the xylem to the shoot, resulting in Fe overload in plant tissues. The excessive accumulation of Fe in plant tissues triggers overproduction of reactive oxygen species (ROS) through the Fenton reaction, causing cellular structural damage and disrupting physiological processes in rice plants (Gupta et al., 2025). Heavy metal Fe exposure in paddy soils induces iron toxicity symptoms in rice, including inhibited root growth, reddish-brown leaf discoloration due to iron plaque deposition, and reduced photosynthetic efficiency, all of which directly affect the quality of the harvested grain (Wairich et al., 2024). The presence of Fe in paddy fields has been documented to elevate Fe concentrations in rice grains (Kabeer et al., 2026).

Pesouha Village in Pomalaa Sub-district, Kolaka Regency, faces direct threats from these environmental hazards. Situated near mining areas and irrigated by rivers originating from mining catchments, Pesouha is exposed to AMD-induced reductions in water pH and the consequent mobilization of heavy metals, particularly iron (Tambara et al., 2025b). According to Okto et al. (2023), Pesouha Village is among the most severely affected areas by red sludge flooding from nickel mine runoff, with approximately 500 hectares of paddy fields inundated, potentially leaving significant heavy metal residues in the agricultural soil.

Kabeer et al. (2026) demonstrated a direct relationship between Fe levels in paddy soils and Fe content in rice grains; however, information on the effect of excessive soil Fe concentrations on grain Fe content in mining-impacted areas remains scarce. Ahadiyat et al. (2023) reported heavy metal accumulation in conventional rice farming systems contaminated by AMD in Indonesia. Zhu et al. (2023) similarly demonstrated that AMD exposure in paddy fields can affect rice quality, heavy metal content in grains, and overall crop productivity. Hu et al. (2025), in a large-scale study analyzing six rice samples, affirmed that heavy metal contamination is site-specific and strongly governed by local environmental conditions. Based on the foregoing, there is a compelling need for integrated research that examines Fe content in AMD-affected paddy soils in relation to Fe concentrations in rice grains and the consequent implications for rice quality.

Although Fe contamination associated with AMD has been reported in several agricultural settings (Li et al., 2023), most existing studies have characterized general heavy metal profiles or have been conducted in regions with markedly different hydrogeochemical and soil management conditions (Haghighizadeh et al., 2024; Zhang et al., 2025), and none have specifically quantified the soil-to-grain transfer of Fe in a nickel-mining-impacted, red-sludge-affected rice landscape such as Pesouha Village a site where Fe contamination in soil and rice has only recently been documented descriptively but not yet linked through a quantitative transfer model (Tambara et al., 2025a). The novelty of the present study therefore lies in providing the first site-specific empirical evidence linking soil Fe status under AMD stress to Fe accumulation in rice grains within a nickel-mining catchment that has received limited prior scientific attention despite documented large-scale flooding by mine-derived red sludge, establishing a quantitative soil-to-grain Fe transfer relationship that can function as an early-warning indicator for food-safety monitoring and land-use decisions in similarly AMD-affected mining regions, and generating baseline data that can support the design of remediation and risk-mitigation strategies for communities relying on rice grown in AMD-contaminated soils (Huang et al., 2024).

By linking soil geochemical behavior under AMD conditions to grain-level Fe accumulation and its agronomic and food-safety implications, this study moves beyond a purely descriptive, localized account of Fe contamination and offers a conceptual and methodological framework that is transferable to other AMD-affected paddy ecosystems.

MATERIALS AND METHODS

Study area

The research was carried out at a study site located at coordinates 4°14′47″ S, 121°41′07″ E in Pesouha Village, which is administratively situated within Pomalaa District (4°10′30″ S, 121°36′53″ E), Southeast Sulawesi, Indonesia (Figure 1).

Sampling location

Sampling points were established in paddy fields adjacent to an irrigation channel contaminated by AMD effluent, comprising four stations: station 1, approximately 200 m from the irrigation channel; station 2, 500 m; station 3, 2 km; and station 4, serving as a control at 4 km from the irrigation channel and receiving irrigation water unaffected by mine waste (Figure 2). A purposive sampling design was applied, with distance from the AMD-affected irrigation channel used as the stratification factor for station placement. At each station, three plots measuring 5 × 5 m and spaced at least 10 m apart were selected. Soil and rice grain samples collected from these plots were pooled to form a single composite sample for each station prior to laboratory analysis. Consequently, four composite samples (one per station) were analyzed for both soil and rice grain parameters.

Assessment of rice plant growth conditions

Direct in situ observations of rice plant growth conditions were performed at each station within the paddy fields, focusing on vegetative growth parameters. The assessed parameters included leaf coloration as an indicator of plant health, plant height, and the morphological condition of leaves and stems. All observations were systematically documented to support descriptive comparative analyses of plant growth conditions across stations.

Analysis of iron content in paddy soils

At each station, three independent composite soil samples (replicates) were collected from the three replicate plots described above, each composite formed by pooling five sub-samples collected in a diagonal (X) pattern within the plot at a depth of 0–20 cm, air-dried at room temperature (25–30 °C), homogenized, and sieved through a 2 mm mesh. Approximately 0.5 g of dried sample was subjected to wet acid digestion using 10 mL of concentrated HNO_3 (65%) at 120 °C, followed by the addition of 3 mL of H_2O_2 (30%) to oxidize residual organic matter and 3 mL of concentrated HCl (37%) to dissolve

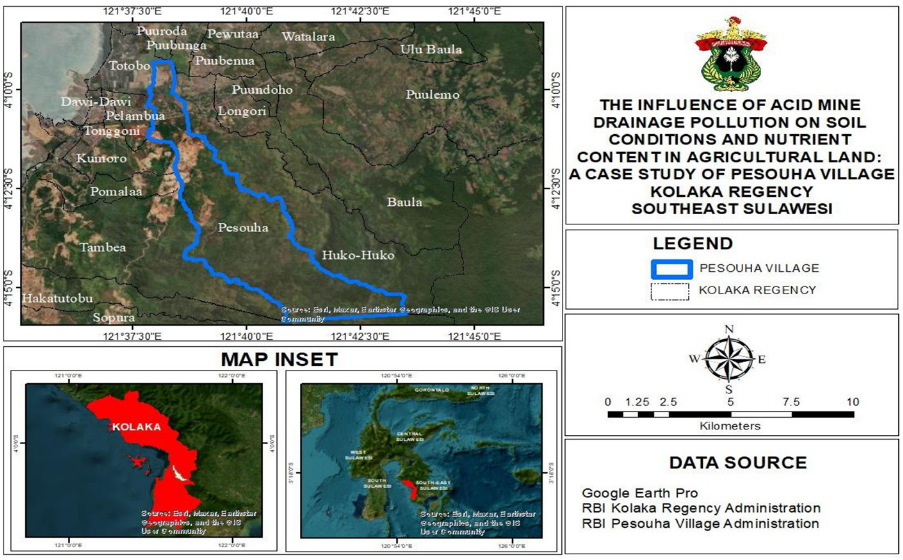

Figure 1. Map of the study area showing the sampling coordinates (adapted from Tambara et al., 2025a)

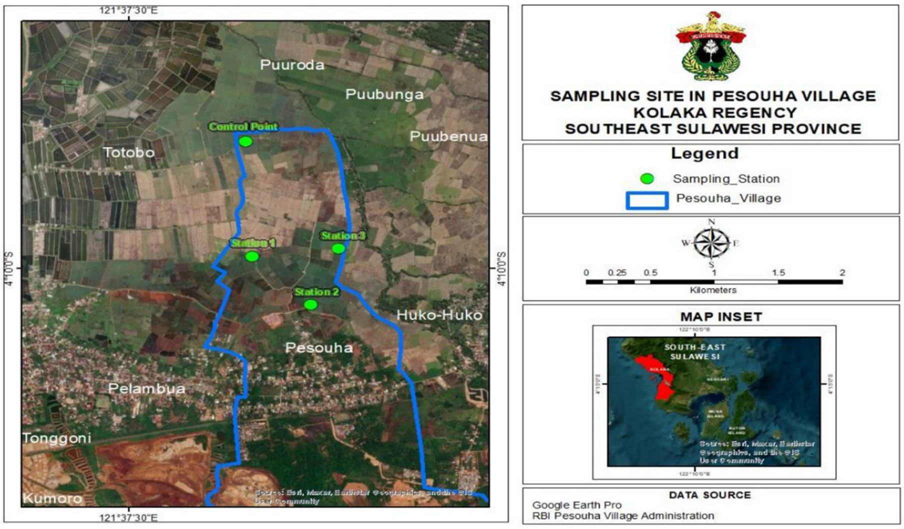

Figure 2. Location of research in the agricultural land of Pesouha Village, Kolaka Regency, Southeast Sulawesi Province (adapted from Tambara et al., 2025a).

metal oxide precipitates, with continued heating at 150 °C until a clear solution was obtained. The digested solution was cooled, filtered through Whatman No. 42 filter paper, and diluted with deionized water to a final volume of 50 mL. Iron concentrations were determined by atomic absorption spectrophotometry (AAS) at a wavelength of 248.3 nm, with each digested sample measured in triplicate (technical replicates); results were expressed as mean ± standard deviation in mg/kg dry weight (mg kg^{-1} dry weight). Quality assurance and quality control (QA/QC) procedures for AAS included calibration with certified standards, reagent blanks, duplicate analyses, and accuracy checks using reference materials and spike recovery tests. Recovery values ranged from 90% to 110%, with calibration curves showing $R^2 > 0.999$.

Rice plant sampling

Rice sampling was conducted at the generative stage, specifically during the grain ripening phase, approximately 105–120 days after transplanting. This stage was identified by the transition of grain color from green to golden yellow and a concurrent decrease in grain moisture content. At each station, samples were collected from the three replicate plots described above; within each plot, 5–10 clumps were randomly selected from observation points following a diagonal (X) pattern and composited into a single representative replicate sample, resulting in a total of 12 rice grain samples (4 stations × 3 replicates).

Sample preparation

Grain panicles were cleaned of soil residues under running water, air-dried, and subsequently oven-dried at 60 °C to constant moisture content. Rice grains were then weighed at 100 g and manually separated from the panicles using gloves. The grain samples were sun-dried until reaching constant moisture content, after which samples of 350–500 g were weighed as dry unhusked grain weight.

Dehusking and grain separation

Paddy grains were carefully dehusked using a mortar and pestle to remove the husk without damaging the rice kernels. The resulting mixture was then winnowed to separate the husk from the rice grains. The separated rice was collected and stored in sealed containers (Figure 3).

Analysis of iron content in rice grains

Rice samples were homogenized and dried at 105 °C to constant weight. Approximately 0.5 g of dried sample was digested using a concentrated HNO_3 and $HClO_4$ mixture. The digested solution was diluted to 50 mL and analyzed for Fe content by atomic absorption spectrophotometry (AAS) at 248.3 nm, with each digested sample measured in triplicate (technical replicates). Results were expressed as mean ± standard deviation in mg/kg dry weight (mg kg^{-1} dry weight). Quality control (QC) for Fe analysis by AAS included a five-point calibration curve (0–8 mg/L Fe) prepared

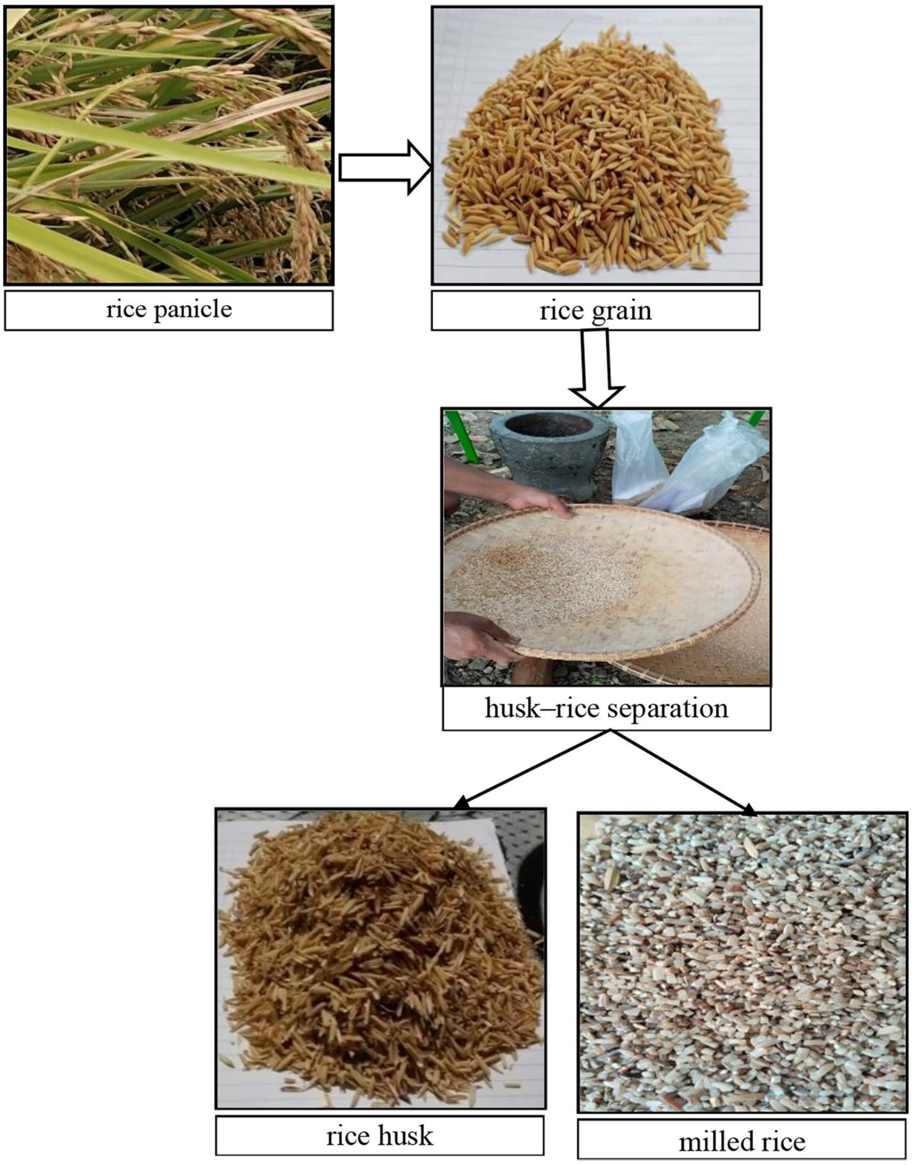

Figure 3. Process of separating rice husk from rice grains

before each run, with only curves showing $R^2 \geq 0.995$ accepted. Reagent blanks and certified reference materials (CRM) were analyzed in each batch to assess contamination and accuracy, with acceptable recoveries of 90–110%. About 10% of samples were analyzed in duplicate, and an RSD <5% was considered acceptable. The LOD and LOQ were calculated from repeated blank measurements. All analyses were performed using flame AAS with an air–acetylene burner.

Assessment of rice grain quality

The physical quality of the harvested rice grains was evaluated with reference to the Indonesian National Standard for milled rice (SNI 6128:2020), including grain moisture content, percentage of broken grains, chalkiness, and the presence of foreign matter or discolored grains. Grain color and translucency were assessed visually against standard rice quality charts. The Fe content of the rice grains was subsequently classified as low, moderate, or high relative to reported ranges for polished/unpolished rice in the literature, in order to evaluate the potential contribution of AMD-affected irrigation water to grain Fe accumulation and its implications for rice quality and consumer safety.

Statistical analysis

For each station, three independent composite samples were collected and analyzed for Fe concentration. Data are expressed as mean ± standard deviation (n = 3 composite samples per station).

Prior to hypothesis testing, the normality and homogeneity of variance of the data were evaluated using the Shapiro–Wilk test and Levene's test, respectively; given the small sample size ($n = 3$ per station), these tests were interpreted with caution as statistical power to detect deviations from normality was limited. Differences in soil and rice grain Fe concentrations among the four stations were analyzed using one-way analysis of variance (ANOVA), followed by Tukey's honestly significant difference (HSD) test for pairwise comparisons when significant differences were observed, with statistical significance set at $p < 0.05$. Pearson correlation analysis was performed to examine the relationship between rice grain Fe content and grain quality score, using station-mean values ($n = 4$ stations).

RESULTS AND DISCUSSION

Paddy field conditions

Field observations revealed that the paddy fields in Pesouha Village are geographically situated in lowland terrain, rendering them highly susceptible to AMD inflow through irrigation channels and surface runoff, particularly during the rainy season. The Pesouha River, which traverses the village and constitutes the principal irrigation source for local agricultural lands, may additionally serve as a conduit for AMD transport into the river system (Figure 4).

Gaber et al. (2025) reported that the use of mine-contaminated irrigation water elevates the iron ion (Fe) concentration in water, potentially diminishing water quality and inhibiting rice plant growth. Beyond Fe, AMD frequently contains other heavy metals such as Cu, Mn, and As, which further compound toxic effects. In Pesouha Village, a considerable portion of the paddy fields exhibited reddish soil discoloration, indicative of iron contamination introduced via AMD through the irrigation system (Figure 5). The oxidation of Fe^{2+} to Fe^{3+} under atmospheric oxygen exposure produces iron oxides such as hematite and goethite, resulting in red-to-brown soil coloration (Syahri et al., 2025; Shabrina et al., 2025).

These conditions manifested in abnormal plant growth, characterized by stunted plants, yellowing leaves indicative of chlorosis, and irregular or absent tiller development (Figure 6). Such symptoms are attributed to heavy metal accumulation disrupting plant physiological systems, including enzymatic activity, photosynthesis, and water and nutrient uptake. Prolonged exposure to Fe and mine-derived chemicals further induces environmental stress that progressively impairs plant growth (Fahruddin et al., 2024; Gaber et al., 2025).

Additionally, the acidic soil conditions enhance the solubility of Fe^{2+} and Fe^{3+}, thereby aggravating phytotoxicity. Low pH conditions also impede the availability of essential nutrients such as phosphorus, potassium, and magnesium, while simultaneously disrupting root metabolism and growth (Yeboah et al., 2021; Thomas and Archana, 2023).

Figure 4. An irrigation canal contaminated by acid mine drainage serves as a water source for rice fields in Pesouhai Village

Figure 5. The rice field soil in Pesauha Village appears reddish-brown in color

Iron content in paddy soils

Analysis of Fe content in paddy soils across all stations yielded values of 3.10 mg/kg at station 1, 2.92 mg/kg at station 2, 2.17 mg/kg at station 3, and 1.19 mg/kg at station 4 (control). These concentrations are considered elevated relative to the permissible thresholds established by the National Standardization Agency of Indonesia (BSN) under SNI 6128:2020 and WHO (2011), which set the Fe limit at >0.5 mg/kg (Figure 7).

Syahri et al. (2025) attributed elevated Fe levels in AMD-contaminated paddy soils to the chemical processes triggered when AMD interacts with soil minerals. Specifically, pyrite oxidation generates sulfuric acid (H_2SO_4) and releases iron, as described by the following reaction:

$$FeS_2 + 3.5O_2 + 4H_2O \rightarrow Fe^{2+} + 2SO_4^{2-} + 4H^+ \quad (1)$$

This reaction yields soluble Fe^{2+} ions, which may subsequently interact with oxygen or microorganisms to produce the more reactive and less soluble Fe^{3+}. The acid generated from pyrite oxidation lowers soil pH, thereby increasing Fe solubility and accelerating the conversion of Fe^{2+} to Fe^{3+}, which then precipitates as iron compounds such as ferrihydrite or goethite. This mechanism commonly drives Fe accumulation in AMD-contaminated paddy soils (Ye et al., 2021; Basri et al., 2024).

Accumulated Fe may either remain as insoluble compounds or be absorbed by plant roots. Elevated soil Fe concentrations can alter soil pH and fertility, and negatively affect plant growth. Furthermore, excess Fe can modify soil structure, impair aeration, and reduce the soil's capacity to sustain optimal plant development (Thomas and Archana. 2023). Notably, station 4 (control) recorded a comparatively lower Fe concentration of 1.19 mg/kg than stations 1, 2, and 3, confirming that paddy fields unexposed to AMD contain lower Fe levels. Nevertheless, even this value exceeds the BSN SNI 19-7117 (2020) and WHO (2011) threshold of >0.5 mg/kg. The relatively elevated Fe in the control station may not be attributable exclusively to AMD, but rather to dissolved iron in irrigation water that has undergone deposition, or prolonged waterlogging of the field, consistent with the findings of Madembo & Nyagumbo (2026), who reported that P fixation in the form of Al-P and Fe-P frequently occurs in rainfed paddies under alternating wet-dry conditions, documented that two soil types with distinct clay mineral compositions naturally contained Fe not as a result of pollution, but as a derivative of the soil parent material.

Rice plant growth at each station

Visual observations across the four stations revealed notable variations in rice plant growth, reflecting differences in environmental conditions and heavy metal accumulation in the paddy soils (Figure 8). At station 1, rice plants grew at an approximately uniform height of 60 cm, with an average of 8 panicles per clump. While some areas displayed relatively sparse plant populations and suboptimal leaf greenness (Thomas and Archana, 2023), the very high Fe concentration of 156 mg/kg likely induced oxidative stress, suppressing plant growth (Sahrawat, 2004). In contrast, Station 2 exhibited highly non-uniform growth, with plant height reduced to approximately 40 cm and markedly few panicles, averaging only 4 per clump. The plants displayed dull straw coloration

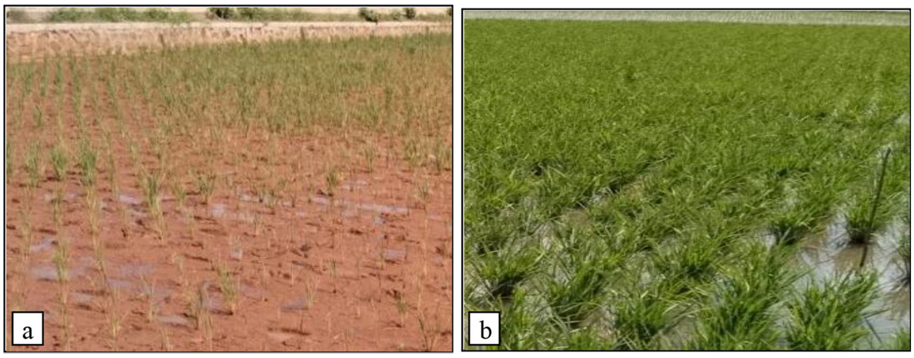

Figure 6. The condition of rice plants in paddy fields: (a) contaminated and (b) not contaminated by mining waste in Pasauha Village.

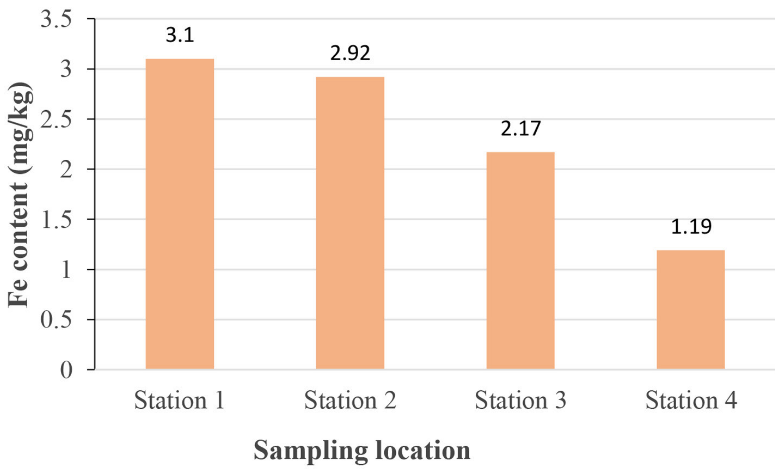

Figure 7. Fe content in paddy soils at each station

and lodging (Gajewska and Skłodowska, 2005). Similarly, station 3 showed chlorosis, suboptimal growth at 45 cm, and low panicle numbers of 5 per clump. The Fe concentration of 50.13 mg/kg at this site further contributed to root growth inhibition and impaired tiller formation (Revathi and Prameela, 2026).

Visual observation of root morphology (Figure 9) revealed clear differences among sampling stations. At Station 1, the roots were short (7 cm in length), sparsely branched, and exhibited a pronounced brownish coloration. This condition is consistent with the high Fe concentration detected in the soil (65,655 mg kg^{-1}), which greatly exceeds the physiological tolerance threshold of most plants and may induce toxic effects. According to Sahrawat (2004)), excessive Fe accumulation promotes the formation of iron plaques on root surfaces, thereby impairing gas exchange and nutrient uptake and ultimately inhibiting root cell elongation.

Stations 2 and 3 exhibited intermediate root development, with root lengths of approximately 15 cm, indicating a slightly better growth performance than that observed at Station 1. This pattern may be associated with differences in heavy metal concentrations, particularly Fe levels, which were 147,360 mg kg^{-1} at Station 2 and 33,440 mg kg^{-1} at Station 3. Nevertheless, the accumulation of other heavy metals, such as Ni and Mn, remained relatively high in these mining waste–contaminated soils. Previous studies have reported that the combined effects of multiple heavy metals can synergistically reduce root enzymatic activity, disrupt normal physiological processes, and hinder optimal root development (Wairich et al., 2024).

In contrast, Station 4 (control site) exhibited healthy root characteristics, including a greater root length (30 cm), extensive branching, and a bright reddish coloration. The Fe concentration at this location (42,400 mg kg^{-1}) was relatively lower than those recorded at the contaminated stations. These conditions likely provided a more stable rhizosphere environment and enhanced tolerance to

Figure 8. The growth of rice plants in paddy fields in Pesouha Village includes: (a) station 1, (b) station 2, (c) station 3, and (d) station 4 as the control

metal-induced stress. This observation is in agreement with Gajewska and Skłodowska (2005), who reported that reduced toxic pressure promotes improved root growth and development.

Station 4 exhibited the most favorable growth, with plants appearing upright, uniformly green, and evenly distributed throughout the plot. Plant height reached 85 cm with an average of 15 panicles per clump. This optimal growth occurred despite a relatively high Fe content of 115 mg/kg, suggesting that other agronomic factors such as soil structure, aeration, and micronutrient availability may have moderated Fe toxicity (Zayed et al., 1998).

These observations collectively indicate that plant height and panicle number, as indicators of growth performance, are substantially influenced by interactions between heavy metals and soil conditions. Excess Fe was negatively associated with plant height and productivity, consistent with the dual behavior of Fe as both an essential micronutrient and a phytotoxic element, depending on its concentration and bioavailability (Kabata-Pendias, 2010).

Iron content in rice grains

Analytical results for Fe content in rice grains yielded values of 156 mg/kg at station 1, 66.67 mg/kg at station 2, 50.13 mg/kg at station 3, and 115 mg/kg at station 4 (control) (Figure 10). The elevated Fe content at station 1 is closely associated with soil conditions at that location. Under flooded paddy conditions, Fe compounds initially in the oxidized ferric state (Fe^{3+}) are reduced to the more soluble ferrous form (Fe^{2+}), which is readily absorbed by rice roots. In waterlogged soils, soluble Fe concentrations can reach 50–100 ppm, far exceeding the approximately 0.1 ppm found in non-waterlogged soils. AMD-contaminated irrigation water further accelerates Fe^{2+} accumulation in paddy soils, facilitating its uptake by rice plants (Becker and Asch, 2005). The introduction of AMD lowers soil pH, and acidic soil conditions significantly enhance Fe absorption and accumulation in rice plants compared to alkaline conditions (Ahadiyat et al., 2023).

According to Kabeer et al. (2026), during the generative phase of rice development, Fe reserves stored in leaves are mobilized and translocated to grains via phloem tissues, resulting in high Fe concentrations in the pericarp and embryo of rice grains. This is consistent with Wairich et al. (2024), who demonstrated that Fe accumulates more readily in soil as Fe^{2+}, which is subsequently absorbed and distributed to grain tissues.

Inter-station variation in rice grain Fe content may also be influenced by the intensity of agricultural activities and local environmental conditions. Elevated soil Fe concentrations were associated with reduced rice yield, where yield decline was directly correlated with Fe^{2+} concentrations in the soil, and iron toxicity at the late vegetative and early reproductive stages caused delayed flowering and impaired grain maturation. Accordingly, the high Fe content in rice at station 1 (156 mg/kg) reflects more intensive accumulation resulting from a

Figure 9. Representative root morphology of 20-day-old rice plants collected from paddy fields in Pesouha Village at (a) station 1, (b) station 2, (c) station 3, and (d) station 4 as the control

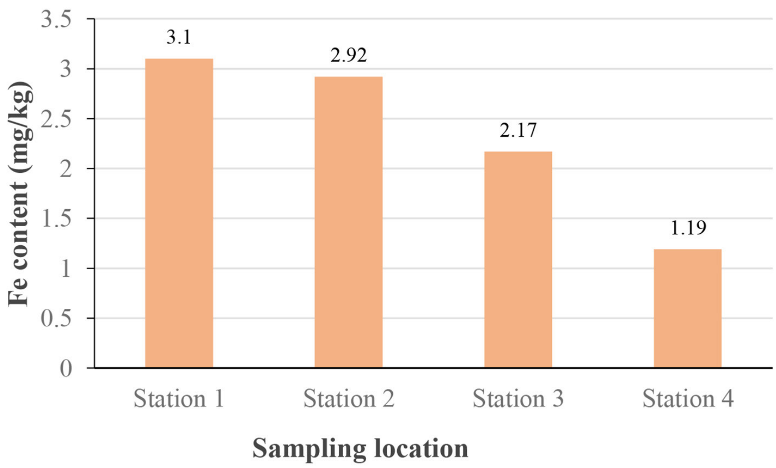

Figure 10. Fe content in rice at each station

combination of distinct soil, hydrological, and environmental factors compared to other stations (Ahadiyat et al., 2023).

The Fe content at station 4 (control), 115 mg/kg, was higher than those at station 2 (66.67 mg/kg) and station 3 (50.13 mg/kg). This may be explained by the presence of competing heavy metals at contaminated stations, such as Zn, Cr, Ni, and Mn, which can compete with or inhibit Fe absorption by plants. Consequently, despite high total heavy metal concentrations in the soil, Fe in grains may be lower at contaminated sites due to competitive ion uptake. Additionally, the high Fe content at station 4 may reflect natural soil conditions that favor Fe bioavailability (Fahruddin et al., 2026; Syakur et al., 2026).

Visual grain quality assessment based on SNI 6128:2020 (Figure 11) indicated that rice at station 1 exhibited relatively bright coloration, fewer broken grains, and slightly yellowish kernels, meeting the criteria for medium-grade rice according to the SNI. The slight yellowish coloration at station 1 may be attributable to physiological stress induced by heavy metal exposure, particularly Fe and Cr, which can disrupt starch formation and reduce grain brightness (Hu et al., 2025). Station 2 rice appeared dull with numerous broken grains, classified as low-quality. Station 3 rice showed numerous grain fractures and darker coloration, also classified as low quality. Station 4 rice exhibited bright color and intact kernels, representing the highest visual quality and supporting premium-grade rice production.

Pearson correlation between Fe content and rice quality

Pearson correlation analysis (Table 1) yielded a correlation coefficient of $r = 0.55$ between Fe content in rice grain and grain quality score, calculated using station-mean values ($n = 4$ stations). This value falls within the range of 0.40–0.599, classified as a moderate positive correlation (Cohen, 1988; Schober et al., 2018); however, this correlation was not statistically significant ($p = 0.450$, $p > 0.05$), likely reflecting the limited statistical power associated with the small number of stations ($n = 4$). The positive direction of this relationship indicates a tendency for grain quality scores to increase with higher Fe content in rice grain, a pattern consistent across the four stations (Table 2): station 4 (Fe = 115 mg/kg) achieved the highest quality score (20, very good), station 1 (Fe = 156 mg/kg) scored 15 (good), station 2 (Fe = 66.67 mg/kg) scored 10 (moderate), and station 3, with the lowest Fe level (50.13 mg/kg), recorded the lowest quality score (8, poor).

The moderate positive correlation ($r = 0.55$) between Fe content in rice grain and grain quality score reflects the dual role of Fe in rice—functioning as both an essential micronutrient and a potentially toxic element at excessive concentrations. Iron is required by rice plants for photosynthesis, cellular respiration, and chlorophyll synthesis (Kobayashi and Nishizawa, 2012 Becker and Asch, 2005), and its accumulation in grain up to a certain level may be associated with better grain filling and quality. Nevertheless, the absence of a strong correlation ($r < 0.70$) indicates

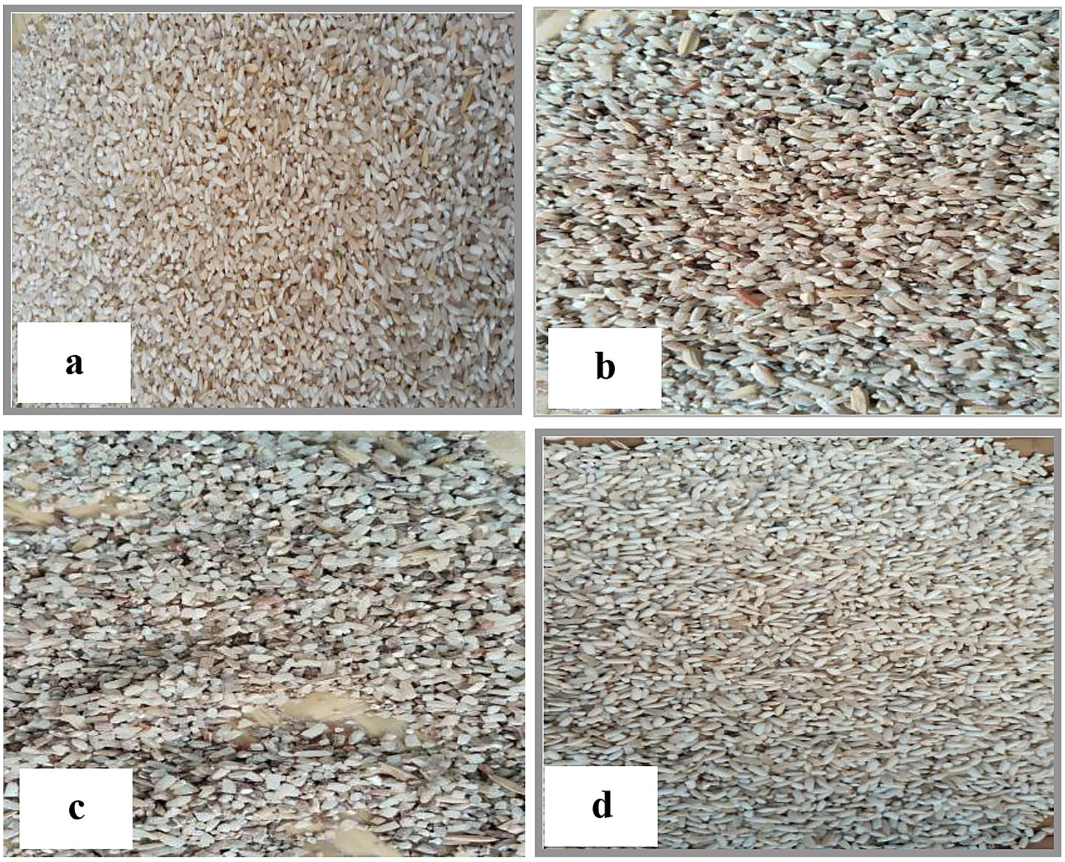

Figure 11. The visual quality of rice from paddy fields in Pesouha Village at each station, namely (a) station 1, (b) station 2, (c) station 3, and (d) station 4 as the control

Table 1. Pearson correlation analysis between Fe content and rice quality score

Variable pair	n	r	95% CI for r	p-value
Fe – Rice quality score	4	0.55	–0.77 to 0.99	0.450 (n.s.)

Note: n.s. = not statistically significant at α = 0.05. Correlation strength benchmark follows Cohen (2013) and Schober et al. (2018); however, strength classification does not substitute for a significance test, particularly at very small sample sizes.

Table 2. Iron (Fe) content and rice quality score at each observation station

Station	Fe (mg/kg)	Rice quality score	Quality category
Station 1	156.00	15	Good
Station 2	66.67	10	Moderate
Station 3	50.13	8	Poor
Station 4	115.00	20	Very Good
Mean ± SD	96.95 ± 48.03	13.25 ± 5.38	–

Note: Source of laboratory analysis results. Quality categories: very good (>18), good (13–18), moderate (8–12), poor (<8). SD = standard deviation.

that the relationship between grain Fe content and quality is not perfectly linear, consistent with threshold-dependent toxicity behavior. At excessively high grain Fe concentrations, such as at station 1 (156 mg/kg), iron toxicity effects – including impaired nutrient uptake and reduced photosynthetic efficiency during grain development (Zhang et al., 2025; Revathi and Prameela, 2026) – may explain why station 1's quality score (15) did not surpass that of station 4 (20) despite its higher Fe content. Given the non-significant correlation ($p > 0.05$) and the small number of stations ($n = 4$), these interpretations should be regarded as preliminary and would benefit from validation using replicate-level (rather than station-mean) correlation analysis or a larger number of sampling stations.

One limitation of this study is the relatively small number of independent sampling stations ($n = 4$). In addition, soil and rice samples were collected using a composite sampling approach, whereby multiple subsamples were combined into a single representative sample for each station. This approach was selected to characterize the average Fe accumulation status of each paddy field exposed to acid mine drainage; however, it does not capture within-site spatial variability. Therefore, the relationships observed between soil Fe and grain Fe concentrations should be interpreted as preliminary and require validation through studies involving a larger number of independent sampling stations and more intensive spatial sampling designs.

CONCLUSIONS

Acid mine drainage from nickel mining caused substantial Fe accumulation in both paddy soils and rice grains at Pesouha Village, Kolaka Regency, with all concentrations exceeding established safety thresholds for agricultural soil and food commodities; soil Fe declined with distance from the contaminated irrigation channel, while grain Fe followed a less consistent pattern reflecting soil geochemistry, competing heavy metals, and site-specific conditions. Rice at AMD-impacted stations showed pronounced iron toxicity symptoms – leaf chlorosis, stunted growth, impaired roots, and reduced panicle formation – and lower grain quality, whereas the uncontaminated control station showed the healthiest growth and highest quality; a moderate, non-significant positive correlation ($r = 0.55$, $p > 0.05$) between grain Fe content and quality score suggests this trend warrants confirmation with more stations or replicate-level analysis. These findings demonstrate that AMD-derived Fe contamination threatens both rice productivity and food safety in mining-affected agricultural zones, underscoring the need for integrated paddy management and continuous irrigation water monitoring.

Although the results demonstrate a relationship between Fe accumulation in paddy soils and rice grains exposed to acid mine drainage, the findings should be interpreted with caution due to the limited number of independent sampling stations and the use of composite sampling. Future studies employing larger sample sizes and more extensive spatial replication are necessary to confirm the observed trends and improve statistical robustness.

Acknowledgements

The authors gratefully acknowledge their supervisors for their valuable guidance and academic support throughout this study. The authors also thank the Director of the Graduate School, Universitas Hasanuddin, for the institutional support provided. We thank the Ministry of Education, Culture, Research, and Technology of Indonesia for funding this research through the PDD 2025 grant (Contract No. 02209/UN4.22/PT.01.03/2025)

REFERENCES

1. Ahadiyat, Y.R., Fauzi, A., Herliana, O., Hadi, S.N. (2023). Mapping heavy metals accumulation in conventional rice farming system at Banyumas Regency of Central Java, Indonesia. *Journal of Degraded and Mining Lands Management* 10(4), 4583–4592, https://doi.org/10.15243/jdmlm.2023.104.4583
2. Badan Standardisasi Nasional (National Standardization Agency of Indonesia). (2020). SNI 6128:2020: Rice. BSN.
3. Basri, S. A. A., Samawi, M. F., Fahruddin, F. (2024). Bioconcentration and translocation of heavy metals in mangrove *Avicennia* sp. and *Rhizophora* sp. in diesel power plant. *Ecological Engineering & Environmental Technology*, *25*(9), 223–230. https://doi.org/10.12912/27197050/190754
4. Becker, M., Asch, F. (2005). Iron toxicity in rice: Conditions and management concepts. *Journal of Plant Nutrition and Soil Science*, *168*(4), 558–573. https://doi.org/10.1002/jpln.200520504
5. Cohen, J. (2013). *Statistical Power Analysis for the Behavioral Sciences (2nd ed.).* Hillsdale, NJ: Lawrence Erlbaum Associates, Publishers. https://doi.org/10.4324/9780203771587
6. Fahruddin, F., Fauziah, S., Samawi, M. F., Johannes, E., Tambaru, E., Abdullah, A. Dwiyanti, L. (2024). Biochar from coconut shell biomass for the removal of sulfate and cadmium reduction in acid mine drainage treatment. *Polish Journal of Environmental Studies, 33*(5), 5627–5634, https://doi.org/10.15244/pjoes/18317
7. Fahruddin, F., Nafie, N.L., Abdullah, A., Tuwo, M., Awaluddin. (2021). Treatment of compost as a source of organic material for bacterial consortium in the removal of sulfate and heavy metal lead (Pb) from acid mine drainage. *Journal of Degraded and Mining Lands Management*, *9*(1), 3083–3091, https://doi.org/10.15243/jdmlm.2021.091.3083
8. Fahruddin, F., Tuwo, M., Samawi, M. (2026). Application of teak leaf biomass-derived biochar into constructed wetlands for sulfate reduction and ph improvement in acid mine drainage-affected aquatic environments. *Egyptian Journal of Aquatic Biology and Fisheries*, *30*(2), 1447–1466. https://doi.org/10.21608/ejabf.2026.454819.7272
9. Gaber, A., Okasha, A., Abdelhamed, M., Zayed, B. (2025). Impact of various irrigation water types on soil quality, grain heavy metals concentration and productivity of some rice varieties. *Journal of Plant Production*, *16*(1), 21–30. https://doi.10.21608/jpp.2025.351258.1428
10. Gajewska, E., Skłodowska, M. (2005). Antioxidative responses and proline level in leaves and roots of pea plants subjected to nickel stress. *Acta Physiologiae Plantarum*, *27*, 329–340. https://doi.org/10.1007/s11738-005-0009-3
11. Gupta, D., Panda, S. K., and Bauer, P., (2025). Meta-analysis of iron excess stress in rice: genes and mechanisms of tolerance to acidic soil. *Physiologia plantarum, 177*(5), e70473. https://doi.org/10.1111/ppl.70473
12. Haghighizadeh, A., Rajabi, O., Nezarat, A., Hajyani, Z., Haghmohammadi, Mina., Hedayatikhah, S., Asl, S., Beni, A. (2024). Comprehensive analysis of heavy metal soil contamination in mining Environments: Impacts, monitoring Techniques, and remediation strategies. *Arabian Journal of Chemistry, 17*, 105777. https://doi.org/10.1016/j.arabjc.2024.105777
13. Hu, F., Wang, B., Wang, Y., Sha, J., Dong, J., Song, H., An, J. (2025). Ecotoxicological effects of heavy metals on rice (*Oryza sativa* L.) Across its life cycle and health risk assessment in soils around Pb-Zn mine. *Plants*, *15*(1), 30. https://doi.org/10.3390/plants15010030
14. Huang, T., Zhou, Y., Yin, S., Deng, D. (2024). Remediation and environmental safety of paddy soil temporarily polluted by heavy metals from acid mine drainage. *Environmental Pollutants and Bioavailability, 36*(1). https://doi.org/10.1080/26395940.2024.2323689
15. Jiao, Y., Zhang, C., Su, P., Tang, Y., Huang, Z., Ma, T. (2023). A review of acid mine drainage: Formation mechanism, treatment technology, typical engineering cases and resource utilization. *Process Safety and Environmental Protection*, *170*, 1240–1260. https://doi.org/10.1016/j.psep.2022.12.083
16. Kabata-Pendias, A. (2010). *Trace elements in soils and plants (4th ed.).* CRC Press. https://doi.org/10.1201/b10158
17. Kabeer, T., Chao, Y., Yufeng, Z., Zengxue, A., Xiaoli, S., Dianxing, W. (2026). Iron biofortification in rice: From iron uptake mechanism to effective breeding. *Rice Science*. Advance online publication. https://doi.org/10.1016/j.rsci.2026.05.003
18. Kobayashi, T., Nishizawa, N.K. (2012). Iron uptake, translocation, and regulation in higher plants. *Annual Review of Plant Biology*, *63*, 131–152. https://doi.org/10.1146/annurev-arplant-042811-105522

19. Li, Q., Han, Z., Tian, Y., Xiao, H., Yang, M. (2023). Risk assessment of heavy metal in farmlands and crops near Pb–Zn mine tailing ponds in Niujiaotang, China. *Toxics*, 11(2), 106. https://doi.org/10.3390/toxics11020106
20. Madembo, C., Nyagumbo, I. (2026). Soil fertility matters most: Rainfed maize productivity under integrated water and nutrient management on granitic sands in sub-humid Zimbabwe. *Agricultural Water Management*, *323*, 110093. https://doi.org/10.1016/j.agwat.2025.110093
21. Okto, A., Rubaiyn, A., Jahidin, La Ode, S., La Ode, A., Asfar, S. (2023). Analysis of groundwater quality in areas surrounding mining sites In Kolaka Regency. *Jurnal Rekayasa Geofisika Indonesia, 5*(1), 1–13, https://doi.org/10.56099/jrgi.v5i01.1
22. Revathi C. and Prameela P., (2026). Iron toxicity and its management in rice: a comprehensive review. *Bhartiya Krishi Anusandhan Patrika, 40*(3), 285–290. https://doi.org/10.18805/BKAP833
23. Sahrawat, K.L. (2004). Iron toxicity in wetland rice and the role of other nutrients. *Journal of Plant Nutrition*, *27*(8), 1471–1504. https://doi.org/10.1081/PLN-200025869
24. Schober, P., Boer, C., Schwarte, L.A. (2018). Correlation coefficients: Appropriate use and interpretation. *Anesthesia & Analgesia*, *126*(5), 1763–1768. https://doi.org/10.1213/ANE.0000000000002864
25. Shabrina, M. H., Fahruddin, F., Samawi, M. F. (2025). Bioaccumulation and translocation of heavy metals mercury and lead in mangroves *Rhizophora apiculata* and *Sonneratia* sp. in the estuarine waters of Malili River. *Ecological Engineering & Environmental Technology*, *26*(4), 88–96. https://doi.org/10.12912/27197050/200653
26. Syahri, Y. F., Mustafa, M., Baharuddin, B., Fahruddin, F., Yani, A., Aswiani, N. (2025). Bacterial potency tests for bioaugmentation in post-mining land. *Journal of Environmental Research, Engineering and Management*, *81*(4), 131–141. https://doi.org/10.5755/j01.erem.81.4.37520
27. Syakur, A., Patandjengi, B., Fahruddin, F., Anshori, M. F., Sofyan, S., Suharman, S., Risal, D. (2026). Indigenous plant growth-promoting rhizobacteria as biofertilizer candidates for hybrid maize in acidic soils. *Journal of Ecological Engineering*, *27*(5), 128–143. https://doi.org/10.12911/22998993/215937
28. Tambara, A., Fahruddin, F., Patandjengi, B. (2025a). Evaluation of the effects of acid mine drainage on soil characteristics and nutrient availability in agricultural land: A case study of Pesouha Village, Kolaka Regency, Southeast Sulawesi. *Journal of Degraded and Mining Lands Management, 12*(4), 8273–8283, https://doi.org/10.15243/jdmlm.2025.124.8273
29. Tambara, A., Fahruddin, F., Patandjengi, B. (2025b). Effect of iron (Fe) concentration on rice field sustainability and paddy growth in Pesouha Village, Pomalaa District, Kolaka Regency. *IOP Conference Series: Earth and Environmental Science*, *1557*, 012017. https://doi.org/10.1088/1755-1315/1557/1/012017
30. Thomas, J., Archana, G. (2023). Differential influence of heavy metals on plant growth promoting attributes of beneficial microbes and their ability to promote growth of *Vigna radiata* (mung bean). *Biocatalysis and Agricultural Biotechnology*, *47*, 102592. https://doi.org/10.1016/j.bcab.2022.102592
31. Titania, O.M., Fahruddin, F., Latunra, A.I. (2026). The potential of coffee husk biochar for chromium removal from acid mine drainage using constructed wetlands. *Journal of Degraded and Mining Lands Management, 13*(1), 9587–9596. https://doi.org/10.15243/jdmlm.2026.131.9587
32. Wairich A., Aung M.S., Ricachenevsky F.K and Masuda, H., (2024). You can't always get as much iron as you want: how rice plants deal with excess of an essential nutrient. *Front. Plant Sci. 15*, 1381856. https://doi.org/10.3389/fpls.2024.1381856
33. World Health Organization. (2011). *Guidelines for drinking-water quality (4th ed.).* WHO Press.
34. Ye, D., Clode, P. L., Hammer, T. A., Pang, J., Lambers, H., Ryan, M. H. (2021). Accumulation of phosphorus and calcium in different cells protects the phosphorus-hyperaccumulator *Ptilotus exaltatus* from phosphorus toxicity in high-phosphorus soils. *Chemosphere*, *264*, 128438. https://doi.org/10.1016/j.chemosphere.2020.128438
35. Yeboah, J., Shi, G., Shi, W. (2021) Effect of Heavy metal contamination on soil enzymes activities. *Journal of Geoscience and Environment Protection*, *9*, 135–154. https://doi.org/10.4236/gep.2021.96008
36. Zayed, A.M., Lytle, C.M., Qian, J.H., Terry, N. (1998). Chromium accumulation, translocation and chemical speciation in vegetable crops. *Planta*, *206*(2), 293–299. https://doi.org/10.1007/s004250050403
37. Zhang, C., Luo, J., Song, W. Han, C., Shunyuan, Z. (2025). Influence of biochar on the partitioning of iron and arsenic from paddy soil contaminated by acid mine drainage. *Scientific Reports, 15*, 4852 (2025). https://doi.org/10.1038/s41598-025-89728-0
38. Zhu, Y., Zhuang, Y., Sun, X., Du, S. (2023). Interactions between cadmium and nutrients and their implications for safe crop production in Cd-contaminated soils. *Critical Reviews in Environmental Science and Technology*, *53*, 2071–2091. https://doi.org/10.1080/10643389.2023.2210985